JOURNAL OF PROPULSION AND POWER
Vol. 16, No. 3, May–June 2000

Nonpremixed Periodic Flames Supported by Heterogeneous Propellants

T. L. Jackson* and J. Buckmaster†
University of Illinois at Urbana–Champaign, Urbana, Illinois 61801

The complex combustion field that is generated by burning a heterogeneous solid propellant of the kind used in high-performance rockets is studied. We consider a propellant whose surface is one-dimensional periodic, generating a two-dimensional combustion field. Two important parameters are the Peclet number *Pe* and the solid-phase stoichiometric coefficient β. We show that for $\beta = 7$, a representative value, there are essentially two flame configurations: For small Peclet numbers, mixing between the surface and the flame is sufficient to generate a continuous and near-uniform deflagration; for Peclet numbers of order 10 or so, each period contains a pair of buttonlike premixed flames centered over the fuel so that there are significant holes in the combustion field over the oxidizer. Diffusion-flame structures that are part of the combustion field play no role in generating the heat that is conducted back to the propellant surface. Most of our calculations assume that both Lewis numbers are equal to 1 and that the solutions are steady, but time-periodic oscillating solutions are obtained for sufficiently large values of Lewis number.

Nomenclature

C_p	= specific heat
D	= Damköhler number
k_X	= fraction of nominal oxidizer that is oxidizer
k_Y	= fraction of binder that is fuel
L	= characteristic (geometric) length
Le	= Lewis number
M	= mass flux
Pe	= Peclet number
Q	= heat of reaction
S	= scaled Z
T_a	= Burke–Schumann flame temperature for the two $\frac{1}{4}$-plane problem
T_w	= wall temperature
X	= mass fraction of oxidizer (gas phase)
x	= distance normal to propellant surface
Y	= mass fraction of fuel (gas phase)
y	= distance parallel to propellant surface
Z	= Schvab–Zeldovich variable (~mixture fraction)
α	= fraction of propellant that is fuel, Fig. 2
α_X, α_Y	= gas phase stoichiometric coefficients
β	= supply stoichiometric ratio
δ	= Damköhler number, De^{-20}
θ	= activation energy
λ	= heat conduction coefficient
$\rho\mathsf{D}$	= mass diffusion coefficient
Ω	= reaction rate

Introduction

THIS is the third in a sequence of elementary flame studies[1] that we believe can contribute to an understanding of the complex combustion field that is generated by burning a heterogeneous solid propellant such as used in high-performance rockets. We are particularly concerned with Ammonium Perchlorate (AP)-in-fuel-matrix propellants.

Stoichiometry considerations require the AP particles to be closely packed,[2] and this can only be accomplished with a variety of particle sizes. Figure 1 shows idealized arrays in which ever smaller particles are placed in the interstices until the appropriate volume fraction is occupied. The necessary ratio of AP volume to fuel matrix volume is of order 10:1.

The nature of the surface of the propellant, the source of oxidizer and fuel fluxes, is defined by cutting the three-dimensional array with a surface that is nominally plane. This surface moves as the propellant erodes, so that at one time it will be located at A (Fig. 1a), at some later time at B. Clearly the surface stoichiometry differs from the volume stoichiometry, so that there will be times when the fluxes from a fixed area are fuel rich and times when they are fuel lean. Because a real propellant will have a stochastic not a periodic nature, it follows that the flux stoichiometry will vary stochastically both in space and in time, and only in an average sense will it have the design volumetric value. Moreover, the nature of the flame structure will vary stochastically. There will, perhaps, be times and places where diffusion flames supported by contiguous streams of fuel and oxidizer exist and times and places where mixing is sufficiently thorough that the local flame structure is essentially that of a deflagration. In due course, three-dimensional flame calculations are needed, and to reach that goal, we study simple two-dimensional configurations of which this is the third. Our fourth contribution will examine the three-dimensional problem.

In Ref. 3 (a preliminary version of which was reported in Ref. 4) we examine sandwich configurations and their axisymmetric counterparts, partly motivated by the experimental studies of Price[5] and his colleagues, e.g. Ref. 5. Buckmaster et al.[3] is concerned for the most part with stationary solutions, but Buckmaster and Jackson[6] consider a flame supported by $\frac{1}{4}$ planes of fuel and oxidizer and calculate the effects of a time-periodic shear flow that is applied parallel to the propellant surface. Significant effects are found on the instantaneous and the time-averaged heat flux to the surface, flux that will significantly affect the regression rate.

Here we consider a plane periodic propellant (Fig. 2). The propellant surface is located at $x = 0$ with fuel Y located in $|y| < \alpha L$ and oxidizer X in $\alpha L < |y| < L$. Periodic boundary conditions are applied at $|y| = L$.

Each portion of the propellant surface is heated, both by conduction directly from the burning gases and by conduction through the propellant. If the surface is hot enough, regression occurs, so that in a frame attached to the surface there is a mass flux of solid/gas from left to right. For a real propellant, this flux will not be uniform in y, and the surface will not remain flat, but in our model we shall ignore this and assign to the flux a constant value M. This is not an approximation to be tested by an examination of the extent to which

Received 28 November 1998; revision received 16 April 1999; accepted for publication 29 April 1999.

*Senior Research Scientist, Center for the Simulation of Advanced Rockets, 1304 West Springfield Avenue; tlj@csar.uiuc.edu.

†Professor, Department of Aeronautical and Astronautical Engineering, 104 South Wright Street; limey@uiuc.edu.

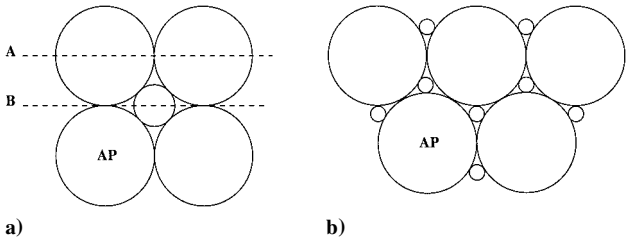

Fig. 1 Idealized propellant packing.

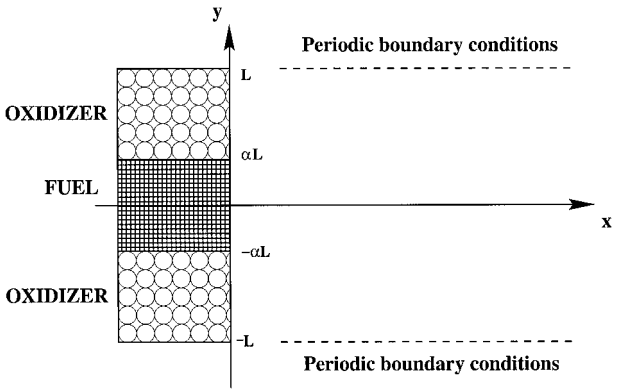

Fig. 2 Plane periodic propellant showing layers of oxidizer (X) and fuel (Y).

it differs from reality, but an ingredient of the model: It is to be tested by the extent to which it gives rise to physically unrepresentative behavior.

The equations that we shall solve in the gas phase ($x > 0$) are

$$M\frac{\partial X}{\partial x} = \rho \mathrm{D}\nabla^2 X - \alpha_X \Omega$$

$$M\frac{\partial Y}{\partial x} = \rho \mathrm{D}\nabla^2 Y - \alpha_Y \Omega \tag{1}$$

where Ω is a reaction rate that we shall discuss later. No two-way coupling between the fluid mechanics and the combustion processes is accounted for, a model ingredient first used by Burke and Schumann[7] in their immortal contribution. However, our treatment differs from that of Burke and Schumann in four ways: 1) we consider plane, rather than axisymmetric geometry; 2) we account for finite chemistry effects; 3) we use flux conditions at the propellant surface, rather than Dirichlet conditions; 4) we preserve the elliptic nature of the problem, retaining streamwise diffusion. The relevance of items 3 and 4 to heterogeneous propellant combustion was perhaps first recognized by Nachbar and Cline[8] and later by Jia and Bilger.[9] The boundary conditions are applied at the propellant surface $x = 0$ and are

$$MX - \rho \mathrm{D}\frac{\partial X}{\partial x} = k_X M \quad \text{or} \quad 0$$

$$MY - \rho \mathrm{D}\frac{\partial Y}{\partial x} = k_Y M \quad \text{or} \quad 0 \tag{2}$$

where the choices depend on whether the surface is oxidizer or fuel. These simply assert that the flux of each gas-phase reactant is an assigned fraction (k_X or k_Y) of the total flux in the solid.

A Schvab–Zeldovich variable (essentially the mixture fraction) is defined by

$$Z = (X/\alpha_X) - (Y/\alpha_Y) \tag{3}$$

where

$$M\frac{\partial Z}{\partial x} = \rho \mathrm{D}\nabla^2 Z \tag{4}$$

with boundary conditions at $x = 0$,

$$MZ - \rho \mathrm{D}\frac{\partial Z}{\partial x} = \begin{cases} (k_X/\alpha_X)M & \text{at oxidizer} \\ -(k_Y/\alpha_Y)M & \text{at fuel} \end{cases} \tag{5}$$

If we nondimensionalize Eqs. (4) and (5) using the length L as a reference length and at the same time write

$$Z = (k_X/\alpha_X)S \tag{6}$$

they become

$$Pe\frac{\partial S}{\partial x} = \nabla^2 S \tag{7}$$

$$x = 0: \qquad S - \frac{1}{Pe}\frac{\partial S}{\partial x} = \begin{cases} 1 & \text{at oxidizer} \\ -\beta & \text{at fuel} \end{cases} \tag{8}$$

where

$$\beta \equiv \alpha_X k_Y / \alpha_Y k_X \tag{9}$$

is the supply stoichiometric ratio. Here, β is significantly greater than 1 for a realistic propellant, much more oxygen is needed than fuel, and following the choice made in Refs. 3, 4, and 6, we shall take $\beta = 7$. $Pe = ML/\rho \mathrm{D}$ is the Peclet number.

If the total fluxes are in stoichiometric proportion we have

$$\frac{M(1-\alpha)k_X}{M\alpha k_Y} = \frac{\alpha_X}{\alpha_Y} \tag{10a}$$

that is,

$$(1-\alpha)/\alpha = \beta \tag{10b}$$

corresponding to $\alpha = \frac{1}{8}$ when $\beta = 7$: A thin slice of fuel lies between two thick slices of oxidizer.

Of particular interest is the stoichiometric level surface (SLS)

$$S = 0 \tag{11}$$

It is characteristic of a diffusion flame that, for all values of the Damköhler number greater than the quenching value, the concentrations of X and Y are small at the flame sheet, which accordingly, if it exists, will lie on the surface $S = 0$.

The location of the SLS can be determined by constructing the Fourier series solution of the system (7) and (8). This solution is

$$S = \sum_0^\infty a_n \cos(n\pi y) e^{\lambda_n x} \tag{12}$$

where

$$\frac{\lambda_n}{Pe} = \frac{1}{2} - \frac{1}{2}\sqrt{1 + \frac{4n^2\pi^2}{Pe^2}} \tag{13a}$$

$$a_0 = -\beta\alpha + (1-\alpha) \tag{13b}$$

$$a_n = -2(1+\beta)\frac{\sin(\alpha n\pi)}{n\pi}\left[1 - \frac{\lambda_n}{Pe}\right]^{-1}, \qquad n \neq 0 \tag{13c}$$

Note that, as $x \to \infty$,

$$S \to a_0 = -\alpha\{\beta - (1-\alpha)/\alpha\} \tag{14}$$

which is positive if $\alpha < 1/(1+\beta)$ (fuel lean) and is negative if $\alpha > 1/(1+\beta)$ (fuel rich). S contours defined by these formulas, including the SLS, are shown in Fig. 3 for $\alpha = \frac{1}{8}$ and $Pe = 5$. Note that the SLS intersects the propellant surface at a value of $|y|$ significantly larger than $\frac{1}{8}$, the boundary between fuel and oxidizer. This is a consequence of the stoichiometry, the demand of the reaction for large amounts of oxidizer, which is an effect first pointed out

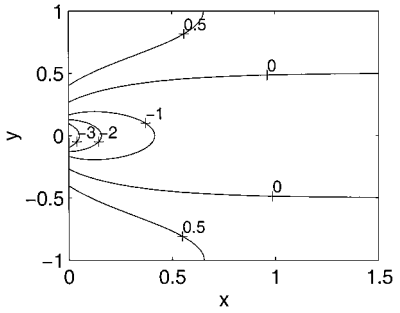

Fig. 3 Level surfaces of S, including the stoichiometric level surface, when $\alpha = \frac{1}{8}$ and $Pe = 5$.

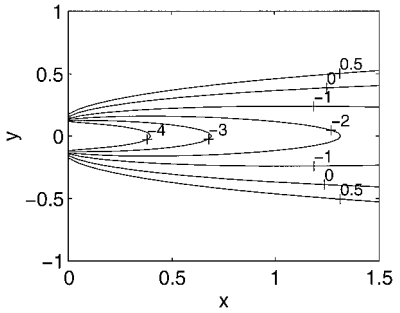

Fig. 4 Level surfaces of S, including the stoichiometric level surface, when $\alpha = \frac{1}{8}$ and $Pe = 40$.

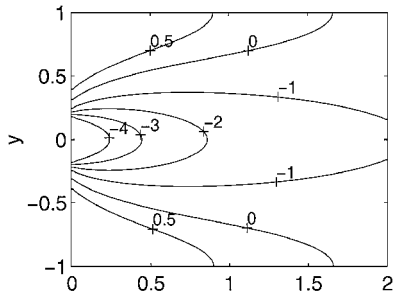

Fig. 5 Level surfaces of S, including the stoichiometric level surface, when $\alpha = 0.2$ and $Pe = 10$.

by Buckmaster et al.[3] and Buckmaster and Yao.[4] The effect diminishes with increasing Peclet number because in the limit $Pe \to \infty$ the boundary conditions (8) become

$$x = 0: \qquad S = \begin{cases} 1 & \text{at oxidizer} \\ -\beta & \text{at fuel} \end{cases} \tag{15}$$

from which it is clear that, in the limit, S changes sign (and so passes through 0) precisely at the fuel/oxidizer junction. However, because of the factor $4\pi^2$ in the discriminant in the formula for λ_n [Eq. (13a)], it takes quite large values of Peclet number to eliminate the shift: It is noticeable even if $Pe = 40$ (Fig. 4). For the sandwich configuration studied by Buckmaster et al.,[3] the shift is more easily eliminated.

Deviations of α from the value $\frac{1}{8}$ lead to overventilated or underventilated configurations, to use language familiar from the classical Burke–Schumann problem. Thus, in Fig. 5 we show contours when $\alpha = 0.2$ and $Pe = 10$, an underventilated (fuel-rich) configuration. A naive interpretation of Fig. 5 would lead to the conclusion that the combustion field consists merely of an array of diffusion flames, each sitting over the oxidizer, with the base of each separated from the base of its immediate neighbor by a distance of 0.6 or so. The reality, however, is quite different, as our finite chemistry calculations make clear.

Finite Chemistry Effects

To account for finite chemistry effects, we return to Eqs. (1) with the choice

$$\Omega = BXYe^{-E/RT} \tag{16}$$

and add the temperature equation

$$C_pM\frac{\partial T}{\partial x} = \lambda\nabla^2 T + QBXYe^{-E/RT} \tag{17}$$

These can be nondimensionalized using the length L (cf. Fig. 2) and the temperature Q/C_p. At the same time we write $X \to \alpha_X X$ and $Y \to \alpha_Y Y$, where

$$\frac{\partial}{\partial x}(X, Y, T) = \frac{1}{Pe}\nabla^2(X, Y, LeT) + (-1, -1, +1)DXYe^{-\theta/T} \tag{18}$$

where

$$Pe = ML/\rho\mathsf{D}, \qquad Le = \lambda/\rho\mathsf{D}C_p$$

$$D = (BL/M)\alpha_X\alpha_Y, \qquad \theta = EC_p/RQ \tag{19}$$

Boundary conditions (2) become

$$X - \frac{1}{Pe}\frac{\partial X}{\partial x} = \frac{k_X}{\alpha_X} \quad \text{or} \quad 0$$

$$Y - \frac{1}{Pe}\frac{\partial Y}{\partial x} = \frac{k_Y}{\alpha_Y} \quad \text{or} \quad 0 \tag{20}$$

and the temperature at the surface is assigned the fixed value T_w.

An important parameter here is the Peclet number. We can reasonably expect that the Peclet number based on a length characteristic of the distance between the reaction center and the propellant surface is of order $\mathcal{O}(1)$, so that convection and diffusion are comparable in the space between the flame and the surface, a standard characteristic of anchored flames. This distance is known to be a few micrometers at the high pressures at which typical rockets are operated. Because AP particle sizes vary from 2 to 100 μm, we conclude, roughly speaking, that Pe varies from $\frac{1}{2}$ to 20. For a Lewis number of 1 (a choice we always make, unless explicitly stated otherwise), we can write $Pe = MLC_p/\lambda$ and then the representative choices[10] $M = 7$ kg/m^2 s, $L = 40\,\mu$m, $C_p = 1.4$ kJ/kg K, and $\lambda = 0.07$ J/ms K define a Peclet number of 5.6.

We have calculated steady solutions as the late time behavior of unsteady solutions using the method of lines, as in Ref. 3. Time derivatives are added to the equations and an unsteady initial-value problem is solved. Discretization in the spatial variables using a sixth-order compact scheme[11,12] leads to a system of ordinary differential equations in time, and these are solved using a low-storage, five-stage, fourth-order accurate Runge–Kutta scheme.[13]

It is clear from the adopted equations that α_Y can be specified arbitrarily, so that k_Y/α_Y can be assigned arbitrarily. Once this assignment is made, k_X/α_X is fixed by the choice of β. This fixes $T_a - T_w$, where T_a is the adiabatic flame temperature, the temperature of a Burke–Schumann flame-sheet supported by two $\frac{1}{4}$ planes of propellant, defined by

$$T_a = T_w + \frac{(k_X/\alpha_X)(k_Y/\alpha_Y)}{(k_X/\alpha_X) + (k_Y/\alpha_Y)} \tag{21}$$

(This temperature is calculated in a standard way by constructing a similarity solution dependent on the variable $y/\sqrt{x}$). Now the temperature ratio $(T_a - T_w)/T_w$ should be assigned some sensible value corresponding to a real flame, and this determines T_w. Alternately, we can arbitrarily assign T_w and work backwards to determine k_Y/α_Y. Thus, with the choice $T_w = 0.2$ and $(T_a - T_w)/T_w = 2$, we have $T_a = 0.6$, $k_Y/\alpha_Y = 3.2$, and $k_X/\alpha_X = 3.2/7$. The nondimensional activation energy is taken to be $\theta = 10T_a = 6$. There are then only two free parameters, the Damköhler number and the Peclet number. We write $D = \delta e^{20}$.

Figure 6 shows reaction-rate contours when $\alpha = 0.2$, $Pe = 10$, and $\delta = 0.1$, the values that define Fig. 5. (The reaction rate is a measure of the heat release.) Note in Fig. 6 that the solid fuel is located in $|y| < 0.2$, the oxidizer is in $0.2 < |y| < 1$, the configuration is periodic in y, and a single period is shown. The strong maxima revealed in Fig. 6 arise because of mixing between the propellant surface and the flame, mixing that enhances the reaction rate over that generated in a pure diffusion flame. Thus, we see that the combustion field consists of a periodic array of premixed structures, each of which is centered over the fuel, weak at the fuel center ($y = 0$), and even weaker at the oxidizer center ($|y| = 1$). More details are apparent in Fig. 7, which shows reaction extending out to $|y| = 1$ in both a weak fuel-lean premixed branch and a weak diffusion-flame branch, the latter following the SLS of Fig. 5. Thus, there exists a tribrachial structure of the kind familiar in unbounded edge-flame studies in which the underlying flame is a diffusion flame,[14] but here the diffusion flame is so weak as to be energetically insignificant. If we focus on the portion of the combustion field for which the reaction rate is ≥ 2 (less than $\frac{1}{3}$ of the maximum), it corresponds to two heat producing lenses per period, each centered at approximately $|y| = 0.4$. Much of the premixed structure lies on the fuel-rich side of the SLS and, consistent with this, excess fuel lies behind it but no oxidizer (Figs. 8a and 8b). Temperature contours are shown in Fig. 8c.

An increase in the Damköhler number drives the flame structure toward the propellant surface and at the same time strengthens

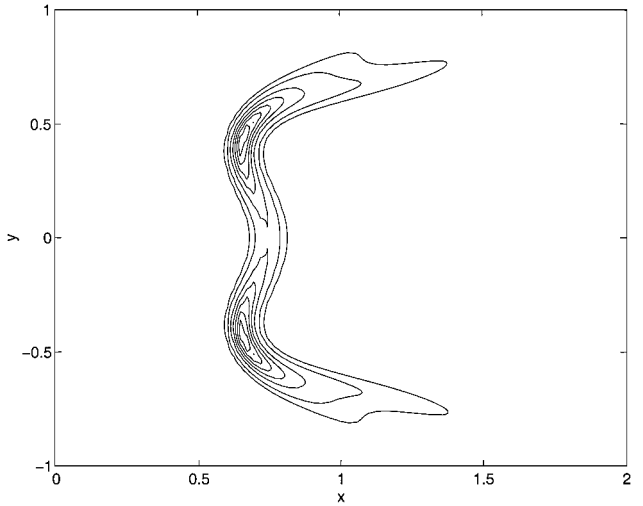

Fig. 6 Contour plot of the reaction rate for $\delta = 0.1$, $Pe = 10$, and $\alpha = 0.2$, with contour levels 6, 5, 4, 3, 2, 1, and 0.5.

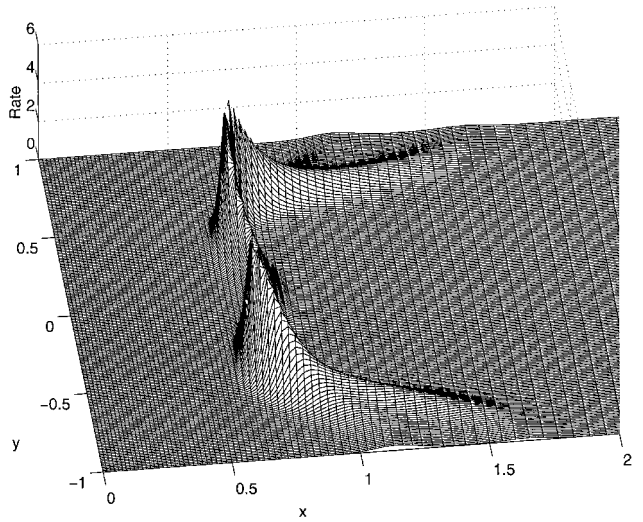

Fig. 7 Surface plot of the reaction rate for $\delta = 0.1$, $Pe = 10$, and $\alpha = 0.2$.

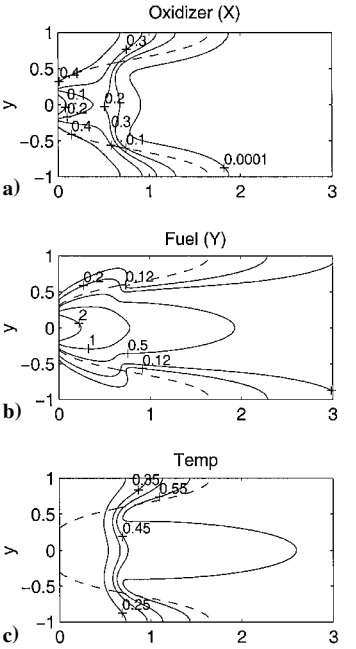

Fig. 8 Contour plots of the solution structure for $Pe = 10$, $\alpha = 0.2$, and $\delta = 0.1$.

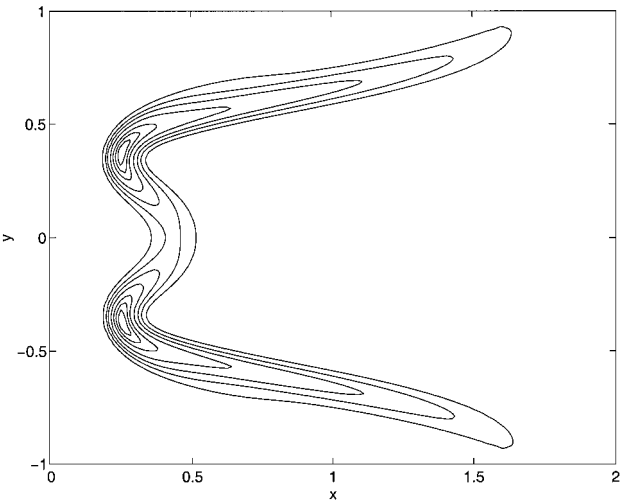

Fig. 9 Contour plot of the reaction rate for $\delta = 0.2$, $Pe = 10$, and $\alpha = 0.2$ with contour values 8, 6, 4, 2, 1, 0.5, and 0.2.

the diffusion flame at the expense of the fuel-lean premixed structure (Figs. 9 and 10). The diffusion flame then plays an important role in heating the gases that pass into the rocket chamber, but the heat flux to the propellant, which controls the regression rate, arises from the premixed structures at the edge (base) of the flame, specifically the fuel-rich branch. Figure 11 is a graph of the surface heat flux for four values of δ. For the smaller δ, the distance between the nonuniform heat source and the surface is quite large, so that the distribution is smoothed, but for $\delta = 0.2$ most of the heat reaches the surface between the oxidizer/binder boundary at $|y| = 0.2$ and a point on the oxidizer surface, $|y| = 0.6$. The flux over the center of the fuel, $y = 0$, is not insignificant, but that over the center of the oxidizer, $|y| = 1$, is. Of course, in reality there is an AP decomposition flame sitting over the oxidizer that heats this part of the propellant.

A decrease of α to 0.1 makes the overall stoichiometry fuel lean (overventilated) so that the SLS closes at $y = 0$ (Fig. 12). But again this plays little role in the combustion field, which is dominated by a premixed structure (Fig. 13d). This flame is essentially fuel-rich,

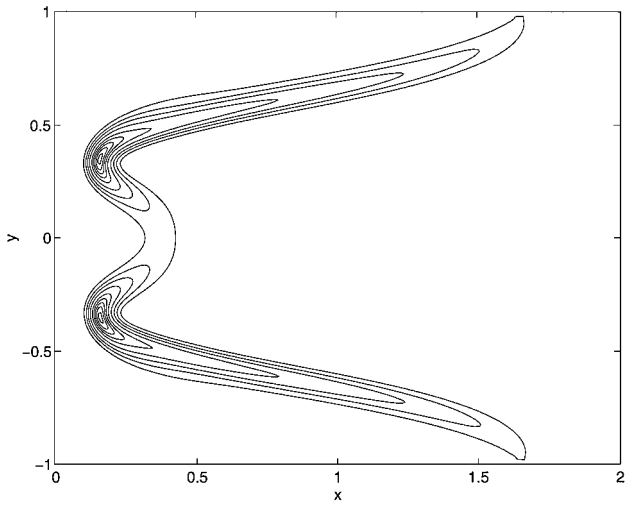

Fig. 10 Contour plot of the reaction rate for $\delta = 0.5$, $Pe = 10$, and $\alpha = 0.2$ with contour values 12, 10, 8, 6, 4, 2, 1, 0.5, and 0.2.

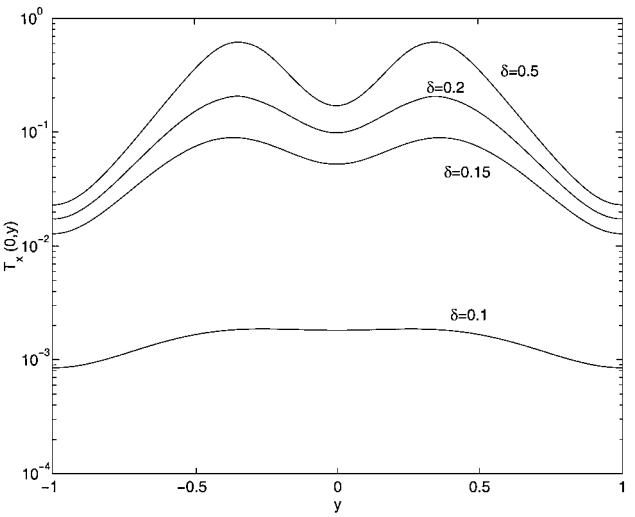

Fig. 11 Heat flux at the propellant surface, $\delta = 0.1$, 0.15, 0.2, and 0.5, $Pe = 10$, and $\alpha = 0.2$.

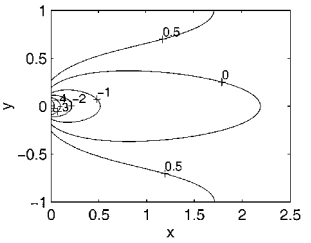

Fig. 12 Level surfaces of S, including the stoichiometric level surface, when $\alpha = 0.1$ and $Pe = 10$.

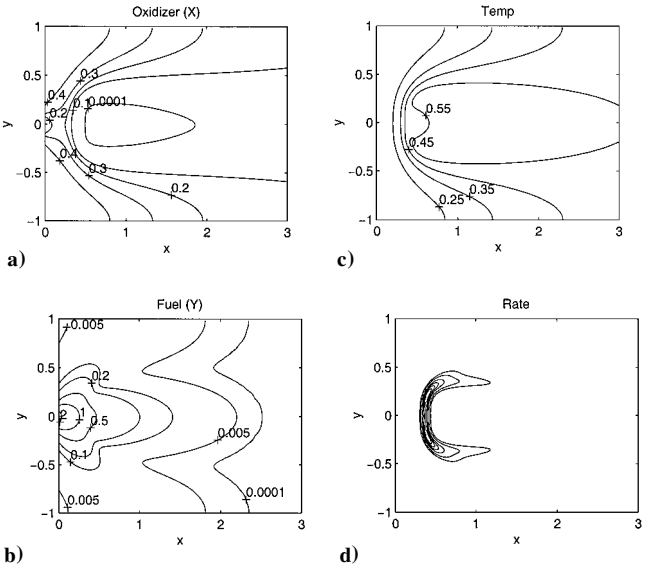

Fig. 13 Contour plots for $Pe = 10$, $\alpha = 0.1$, and $\delta = 0.1$ with contour levels for the reaction rate 5, 4, 3, 2, 1, and 0.5.

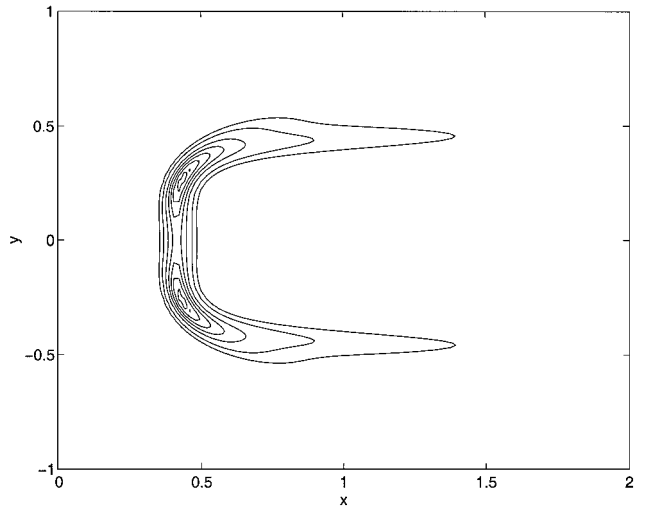

Fig. 14 Contour plot of the reaction rate for $Pe = 10$, $\alpha = 0.125$, and $\delta = 0.1$ with contour levels 6, 5, 4, 3, 2, 1, and 0.5.

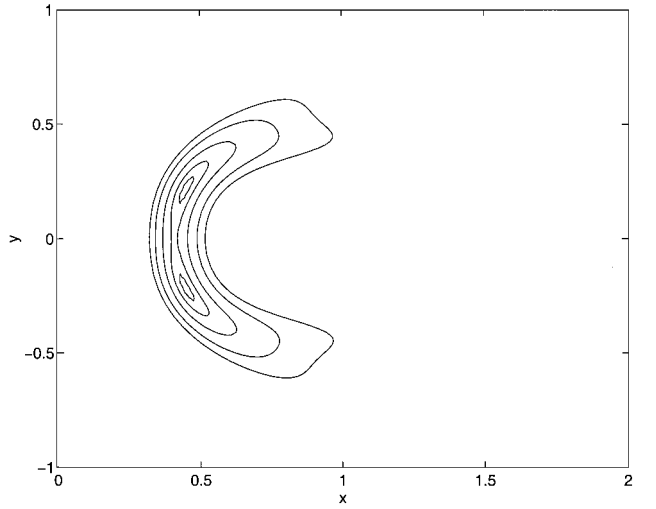

Fig. 15 Contour plot of the reaction rate for $Pe = 5$, $\alpha = 0.125$, and $\delta = 0.1$ with contour levels 3.5, 3, 2, 1, and 0.5.

despite the overall stoichiometry (Figs. 13a and 13b). Again, a striking feature of the solution is how little of the heat generated at the flame can reach the core of the oxidizer centered at $|y| = 1$. This is also true under stoichiometric conditions ($\alpha = \frac{1}{8}$), when $Pe = 10$ (Fig. 14), and is a consequence of β being significantly greater than 1.

Decreasing the Peclet number gives rise to a greater amount of mixing between the flame and the surface. At the same time, with the Damköhler number fixed, the reacting structure thickens (Fig. 15). A one-dimensional premixed structure extending over the entire interval can be generated for small Peclet numbers, for example Figs. 16 and 17.

A striking feature of our results is the "hole" that appears over the oxidizer when the Peclet number is not small. This is a consequence of β being greater than 1. Figure 18 shows reaction rate contours

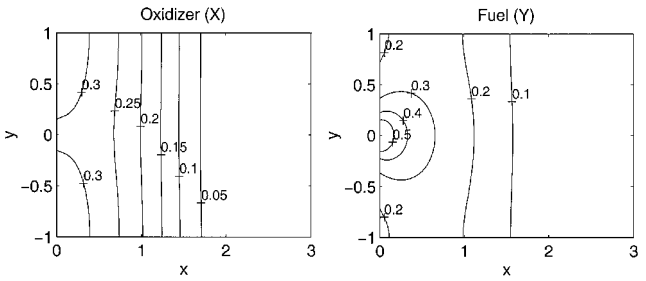

Fig. 16 Contour plot of the oxidizer and fuel for $Pe = 1$, $\alpha = 0.125$, and $\delta = 0.1$.

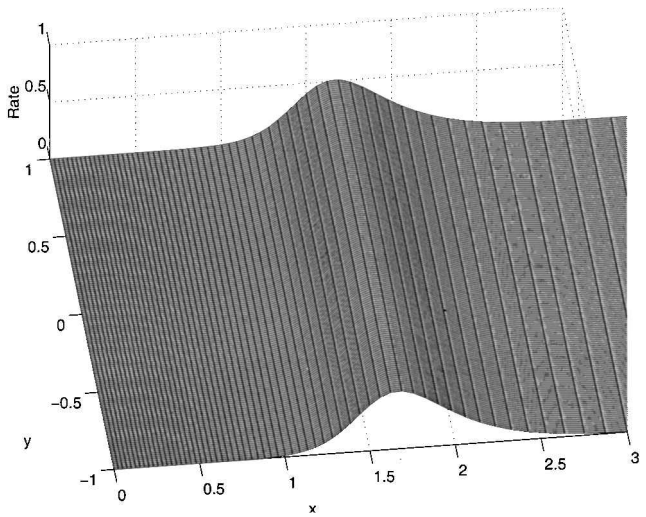

Fig. 17 Surface plot of the reaction rate for $Pe = 1$, $\alpha = 0.125$, and $\delta = 0.1$.

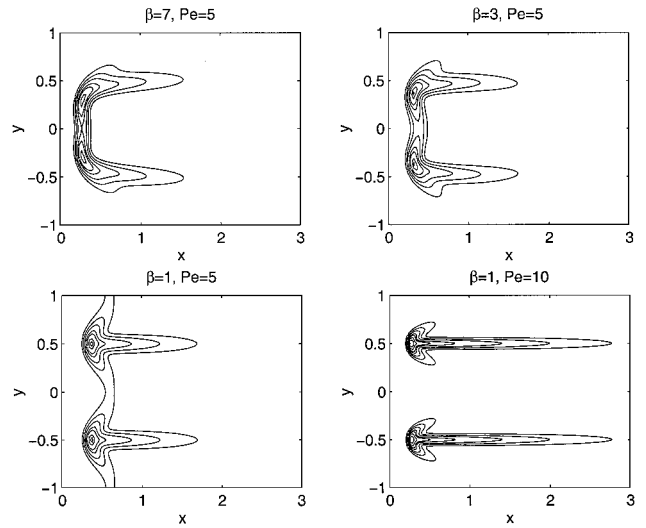

Fig. 18 Contour plot of the reaction rate for various values of β at stoichiometry so that $\alpha = 1/(1+\beta)$ and $\delta = 0.5$ with contour values: ($\beta = 7$, $Pe = 5$) 5, 3, 2, 1, 0.5, and 0.2; ($\beta = 3$, $Pe = 5$) 6, 5, 3, 2, 1, 0.5, and 0.2; ($\beta = 1$, $Pe = 5$) 6, 5, 3, 2, 1, 0.5, and 0.2; and ($\beta = 1$, $Pe = 10$) 11, 8, 5, 3, 2, 1, 0.5, and 0.2.

for various values of β when α is assigned the stoichiometric value $1/(1+\beta)$. When $\beta = 1$ ($\alpha = \frac{1}{2}$), there is no distinction between fuel and oxidizer and the $y-$period is equal to 1. Premixed structures sit over the points $|y| = \frac{1}{2}$, quite intense structures when $Pe = 10$, and the reaction weakening over the center of the oxidizer is identical to the reaction weakening over the center of the fuel. However, when β is increased, the weakening over the oxidizer is much greater than that over the fuel.

Oscillating Flames

It is well known that premixed flames are subject to oscillating instabilities when an appropriate Lewis number is sufficiently large[15] and that this instability is exacerbated by heat losses to a holder.[16,17] Note, in particular, that Buckmaster[17] uses the same boundary conditions as here, albeit in the premixed context, and this work shows that it is possible to excite the instability even if $Le = 1$. In examining the premixed structures that are such a significant ingredient of the present solutions, it is natural to wonder if they might oscillate at certain operating conditions. This is not a matter that can be explored in any depth in the absence of a more realistic reaction-diffusion model than the present one because the values of the transport coefficients, the mass efflux from the propellant surface, and the flame stand-off distance all play important roles in defining any instability. However, we thought it would be of interest to do a few calculations with Lewis number bigger than 1, to see what that would yield. Strong oscillations are found when $Pe = 1$, $Le = 1.6$, and $\alpha = \frac{1}{8}$ ($\beta = 7$). Stronger still are the oscillations when $Le = 2$, but they can be suppressed by increasing the Peclet number. Thus, in Fig. 19, we see variations in the maximum temperature with time for different values of Peclet number. No instability is seen when $Pe = 4$. Whether or not oscillations occur also depends on the value of α. In Fig. 20, we see the variations of maximum temperature for $\alpha = 0.1$, 0.2, and 0.4. Oscillations are suppressed when $\alpha = 0.08$ and when $\alpha = 0.5$, far from stoichiometry, an unsurprising result because the premixed structures are then weakened. The total heat flux to the surface (integrated over the spatial period) can fluctuate significantly during these oscillations (Fig. 21).

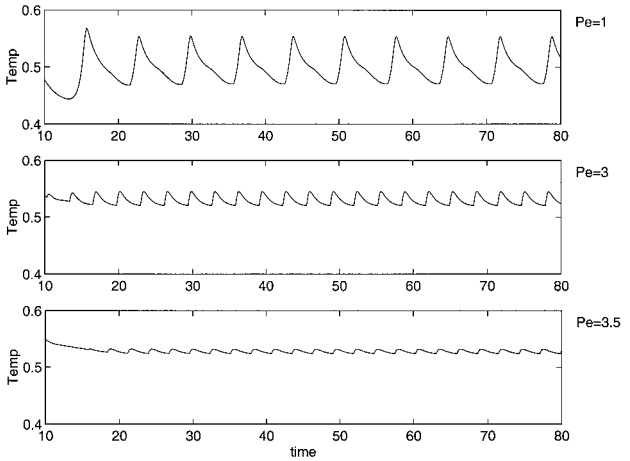

Fig. 19 Temporal variations of maximum temperature when $Le = 2$, $\delta = 0.1$, $\alpha = \frac{1}{8}$, and $Pe = 1$, 3, and 3.5 (top to bottom).

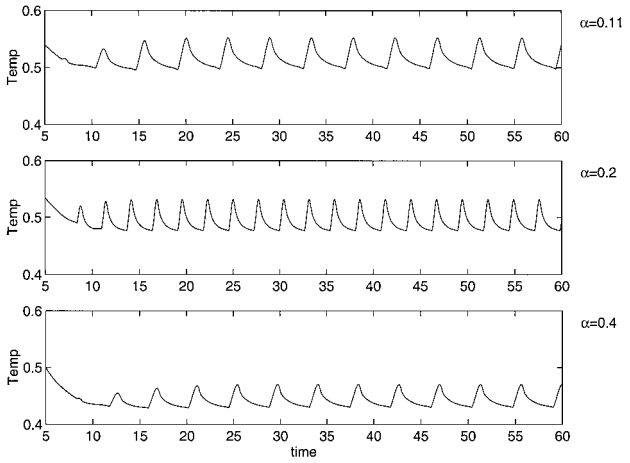

Fig. 20 Temporal variations of maximum temperature when $Le = 2$, $Pe = 3$, $\delta = 0.1$, and $\alpha = 0.11$, 0.2, and 0.4.

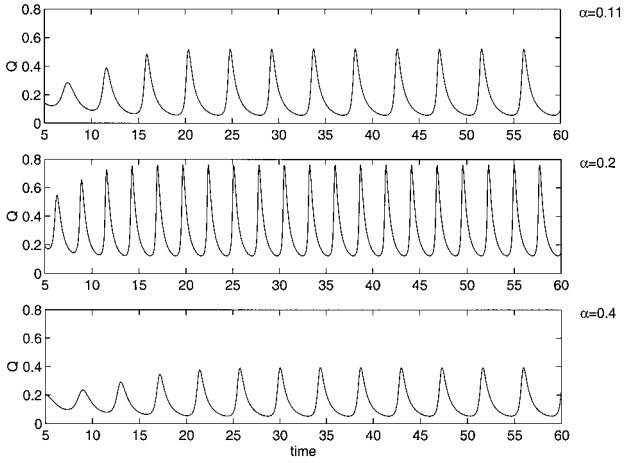

Fig. 21 Temporal variations of the total surface heat flux when $Le = 2$, $Pe = 3$, $\delta = 0.1$, and $\alpha = 0.11, 0.2$, and 0.4.

Conclusions

We have described flame structures defined by a simple model of a periodic heterogeneous propellant. These results, like those of Buckmaster et al.[3] and Buckmaster and Yao[4] establish the importance of the Peclet number in controlling the nature of the combustion field. Thus, when Peclet number is small, the flame is indistinguishable from a one-dimensional deflagration. This result is intuitively unsurprising, but we also find that for Peclet numbers of order 10, although one dimensionality is lost, premixed structures dominate and provide the heat that, conducted back toward the propellant surface, is responsible for the regression. The importance of edge structures in this connection is also apparent in the results of Buckmaster et al.[3] and provides strong evidence justifying the claims that Price[5] has made over the years of the importance of the edge flame.

Inhomogeneities in the combustion field, variations in the direction parallel to the propellant surface, are striking when realistic choices are made for the reaction stoichiometry. Reaction (and, therefore, heat generation) is concentrated over that portion of the oxidizer that is close to the fuel, and there is a significant hole in the flame, centered at the center of the oxidizer. This will obviously have an impact on how the regression rate varies over the surface. Of course, the regression rate, which in our model is fixed, will also be affected by the AP decomposition flame, something that we do not consider.

There appears to be little if any work that addresses the question of what the important Lewis numbers are and what their magnitudes are in propellant flames, although recent efforts to wrestle with realistic propellant kinetics offer promise for the future. However, we note that there is a possibility that, should real propellants have suitable parameter values, oscillating instabilities of the premixed structures could occur, creatures of the Lewis numbers and the heat loss from the structures to the propellant. In the context of our elementary model, we are able to generate oscillations of this nature.

Finally, the preliminary explorations whose results are recorded here and in Refs. 3, 4, and 6 need now to be enlarged to incorporate more realistic configuration. The list of ingredients is formidable, including three-dimensional effects, flow coupling, complex kinetic modeling, coupling with the thermal processes in the solid, etc., but we anticipate that progress will be made in these areas in the future.

We are of course aware that an examination of the regression rate defines what is sometimes called an eigenvalue problem, reflecting that this rate is to be determined simultaneously with the calculation of the combustion field in the gas and the thermal field in the solid. The rubric eigenvalue is not a good one for the one-dimensional problem, and it is even less appropriate for the multidimensional problem where, in fact, the determination of the location of the propellant surface defines a free-boundary problem. However, the surface-averaged regression rate is a one-dimensional concept, and obviously simple models could be constructed in which the gas phase calculations presented here are coupled to a solid-phase description, and this average regression is calculated. There seems little point in doing this, however, without accounting for the heat generated by the AP decomposition flame and without adopting kinetic parameters that reasonably reflect real propellants.

Acknowledgment

The work of J. Buckmaster is supported by the U.S. Office of Scientific Research, by BMDO/ONR under MURI Grant N00014-95-1-1339 to the University of Illinois and by the U.S. Department of Energy through the University of California under Subcontract B341494. T. L. Jackson is supported by the latter agency.

References

[1]Buckmaster, J., and Jackson, T. L., "Response of Propellant Flames to Unsteady Flows, and Related Questions," AIAA Paper 99-0323, Jan. 1999.

[2]Sutton, G. P., *Rocket Propulsion Elements*, 6th ed., Wiley, New York, 1992, p. 450.

[3]Buckmaster, J., Jackson, T. L., and Yao, J., "An Elementary Discussion of Propellant Flame Geometry," *Combustion and Flame*, Vol. 117, No. 3, 1999, pp. 541–552.

[4]Buckmaster, J., and Yao, J., "Flame Configurations in Heterogeneous Propellants," *Proceedings of the Fourth Asian-Pacific International Symposium on Combustion and Energy Utilization*, Vol. 1, Energy Research Inst. and Faculty of Engineering, Chulalongkorn Univ., Bangkok, Thailand, 1997, pp. 112–115.

[5]Price, E. W., "Effect of Multidimensional Flamelets in Composite Propellant Combustion," *Journal of Propulsion and Power*, Vol. 11, No. 4, 1995, pp. 717–728.

[6]Buckmaster, J., and Jackson, T. L., "The Effects of Time-Periodic Shear on a Diffusion Flame Anchored to a Propellant," (submitted for publication).

[7]Burke, S. P., and Schumann, T. E. W., "Diffusion Flames," *Industrial and Engineering Chemistry*, Vol. 20, No. 4, 1928, pp. 998–1004.

[8]Nachbar, W., and Cline, G. B., "The Effects of Particle Size and Non-Stoichiometric Composition on the Burning Rates of Composite Solid Propellants," *Combustion and Propulsion, Fifth AGARD Colloquium*, edited by R. P. Hagerty, A. L. Jaumote, O. Lutz, and S. S. Penner, Pergamon, Oxford, England, UK, 1963, pp. 551–568.

[9]Jia, X., and Bilger, R. W., "The Burke–Schumann Diffusion Flame with Zero Net Flux Boundary Conditions," *Combustion Science and Technology*, Vol. 99, No. 2, 1988, pp. 371–376.

[10]Ward, M. J., Son, S. F., and Brewster, M. Q., "Role of Gas- and Condensed-Phase Kinetic in Burning Rate Control of Energetic Solids," *Combustion Theory and Modelling*, Vol. 2, No. 3, 1998, pp. 293–312.

[11]Lele, S. K., "Compact Finite Difference Schemes with Spectral-Like Resolution," *Journal of Computational Physics*, Vol. 103, No. 1, 1992, pp. 16–42.

[12]Carpenter, M. H., and Kennedy, C. A., "Fourth-Order 2N-Storage Runge–Kutta Schemes," NASA TM 109112, 1994.

[13]Carpenter, M. H., Gottlieb, D., and Abarbanel, S., "The Stability of Numerical Boundary Treatments for Compact High-Order Finite-Difference Schemes," *Journal of Computational Physics*, Vol. 108, No. 2, 1993, pp. 272–295.

[14]Kioni, P. N., Rogg, B., Bray, K. N. C., and Liñán, A., "Flame Spread in Laminar Mixing Layers: The Triple Flame," *Combustion and Flame*, Vol. 95, No. 2, 1993, pp. 276–290.

[15]Williams, F. A., *Combustion Theory*, 2nd ed., Benjamin/Cummings, Menlo Park, CA, 1985, p. 341.

[16]Margolis, S. B., "Bifurcation Phenomena in Burner-Stabilized Premixed Flames," *Combustion Science and Technology*, Vol. 22, No. 1, 1980, pp. 143–169.

[17]Buckmaster, J., "Stability of the Porous Plug Burner Flame," *Journal of Applied Mathematics*, Vol. 43, No. 6, 1983, pp. 1335–1349.